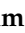




Article

Evaluation of Alkaloids Isolated from *Ruta graveolens* as Photosynthesis Inhibitors

Olívia Moreira Sampaio ¹, Lucas Campos Curcino Vieira ², Barbara Sayuri Bellete ³,
Beatriz King-Diaz ⁴, Blas Lotina-Hennsen ⁴, Maria Fátima das Graças Fernandes da Silva ⁵
and Thiago André Moura Veiga ^{6,*}

¹ Department of Chemistry, Federal University of Mato Grosso, Cuiabá-MT 78068-600, Brazil; ollysampa@ufmt.br

² Engineering Institute, Federal University of Mato Grosso, Várzea Grande-MT 78060-900, Brazil; lucascurcino@gmail.com

³ Department of Chemistry, Federal University of Lavras, Minas Gerais-MG 37200-000, Brazil; barbarabellete@gmail.com

⁴ Department of Biochemistry, University Nacional Autonoma de Mexico, Mexico City 04510, Mexico; kingbeat@unam.mx (B.K.-D.); blas@unam.mx (B.L.-H.)

⁵ Department of Chemistry, Federal University of São Carlos, São Carlos-SP 13565-905, Brazil; dmfs@ufscar.br

⁶ Department of Chemistry, Federal University of São Paulo, Diadema-SP 09972-270, Brazil

* Correspondence: tveiga@unifesp.br; Tel.: +55-11-4044-0500

Academic Editor: John C. D'Auria

Received: 12 September 2018; Accepted: 6 October 2018; Published: 19 October 2018



Abstract: Eight alkaloids (1–8) were isolated from *Ruta graveolens*, and their herbicide activities were evaluated through in vitro, semivivo, and in vivo assays. The most relevant results were observed for Compounds 5 and 6–8 at 150 µM, which decreased dry biomass by 20% and 23%, respectively. These are significant results since they presented similar values with the positive control, commercial herbicide 3-(3,4-dichlorophenyl)-1,1-dimethylurea (DCMU). Based on the performed assays, Compound 5 (graveoline) is classified as an electron-transport inhibitor during the light phase of photosynthesis, as well as a plant-growth regulator. On the other hand, Compounds 6–8 inhibited electron and energy transfers, and are also plant-growth inhibitors. These phytotoxic behaviors based on acridone and quinolone alkaloids may serve as a valuable tool in the further development of a new class of herbicides since natural products represent an interesting alternative to replace commercial herbicides, potentially due their low toxicity.

Keywords: *Ruta graveolens*; photosystem II; Chl *a* fluorescence; Hill reaction inhibitors; acridone alkaloids

1. Introduction

Ruta graveolens L. (Rutaceae) is a medicinal plant whose roots and aerial parts contain more than 120 special metabolites as coumarins, flavonoids, acridones, and furoquinoline alkaloids [1,2]. Many of these metabolites have attracted biological and pharmacological interest, demonstrating antifungal, phytotoxic, and antidotal activities [3–9]. In this context, the effect of the natural products as photosynthesis inhibitors has been efficiently evaluated [10–12]. The photosynthetic process is divided into three parts: the initial light-harvesting process and local charge separation, proton-coupled electron transfer, and multielectronic redox catalysis [13]. During the phenomenon, light absorption by antenna molecules is followed by efficient charge separation across the membrane via photosynthetic reaction centers [14]. The antenna system absorbs and converts light into chemical energy at P₆₈₀. Accordingly, charge recombination is prevented by the presence of an electron-transport chain driving electrons towards P₇₀₀; a second light-harvesting process occurs at photosystem I (PSI),

providing additional energy to electrons for their final purpose: production of adenosine triphosphate (ATP) and dihydronicotinamide-adenine dinucleotide phosphate (NADPH), which are used for CO₂ fixation through the Calvin cycle (biochemistry phase) [13,14]. Therefore, we analyzed chlorophyll *a* fluorescence kinetic transients to verify the damage on photosynthetic apparatus, demonstrating the quantitative and qualitative effects of herbicides on both photosystems [15,16]. From this perspective, the main goal of this report was to investigate the effects of alkaloids (1–8) isolated from *Ruta graveolens* L. (Figure 1) on photosynthetic activities through polarography, chlorophyll (Chl) *a* fluorescence, and in vivo plant-growth experiments. Our results suggested that these techniques are powerful and sensitive enough to localize, in detail, the mechanisms of action related to such a complex target, photosynthesis.

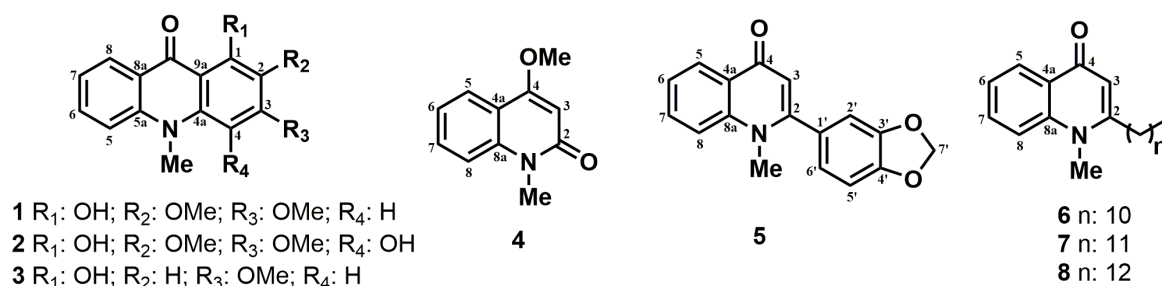


Figure 1. Alkaloids isolated from *Ruta graveolens*.

2. Results and Discussion

2.1. Effect of Alkaloids 1–8 on Noncyclic Electron Transport and H⁺-ATPase Activity

Compounds 2 and 3 did not present an effect on noncyclic electron transport in preliminary tests. On the other hand, the other alkaloids inhibited noncyclic electron transport from H₂O to methylviologen (MV) in chloroplasts isolated from *Spinacea oleracea* L. Arborinine (1) inhibited phosphorylating and uncoupled electron flow by 100% at 100 μM, which demonstrated that (1) behaves as a potent electron-transport inhibitor (Figure 2A). The basal electron flow was increased at low concentrations (around 15 μM), but electron flow at concentrations higher than 25 μM was decreased, inhibiting electron flow by 20% at 100 μM, which means that (1) binds to the CF₁CF₀-ATPase complex, suggesting inhibitory activity on ATP synthesis. The results found, with regard to electron-transport reaction, a increment of the step as well as a decrease in the phosphorylating and uncoupled steps, indicating that (1) exhibited a dual effect by inhibiting both energy transfer and electron transport [17].

Compound 4 increased basal and phosphorylating electron transports by 80% and 40%, respectively, at the beginning of the illumination, and then decreased them, since the concentrations were higher than 80 μM (Figure 2B). As well as Compound (1), (4) decreased the uncoupled phase at concentrations close to 80 μM. Therefore, (4) did not demonstrate electron-transport inhibition, but rather acted as a decoupling agent. Graveoline (5) inhibited the basal, phosphorylating, and uncoupled electron transport by 40% at 300 μM, which suggested Hill reaction inhibitory behavior (Figure 2C).

Homolog mixture 6–8 inhibited energy transfer at 25 μM and showed slight inhibitory activity on electron-transport reactions at concentrations up to 100 μM (Figure 2D). Compounds 6–8 increased basal and phosphorylating electron transport by 230% and 140%, respectively. The uncoupled electron transport showed a small increase in concentrations below 100 μM. In this way, the mixture behaved mainly as an energy-transfer inhibitor and showed electron-transport inhibitory activity at higher concentrations.

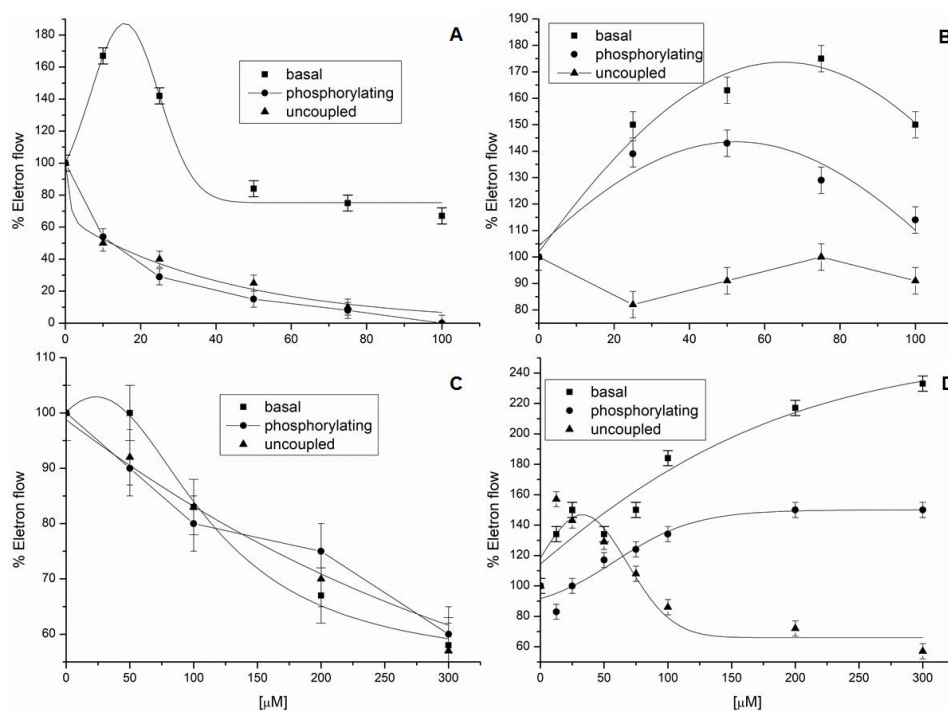


Figure 2. Effect of the alkaloids isolated from *R. graveolens* on electron flow. Control-rate values for electron transport from basal, phosphorylating, and uncoupled conditions were 450, 620, and 1200 $\mu\text{equiv e}^{-} \text{h}^{-1} \text{mg}^{-1} \text{Chl}^{-1}$, respectively. Panel (A): Compound 1; Panel (B): Compound 4; Panel (C): Compound 5; and Panel (D): Mixtures 6–8.

When there is a significant increase on the basal electron-transport step, as observed for Compounds 1, 4, and 6–8, this is an indication that the compounds are acting on the ATP–synthase complex [17]. Cyclic electron transport is happening normally, as can be observed in the basal reaction, due the behavior of the chloroplasts in the reaction medium. The percentage of the basal curve means that the effect is happening over the ATP–synthase complex once the basal reaction works harder to equilibrate this damage, thus increasing the speed of action.

Due to this, ATPase analysis for Compounds 1, 4, and 6–8 was needed to confirm if they interfere on the CF_1CF_0 -ATPase complex, acting by direct inhibition of ATP synthesis. The experiments (Table 1) revealed that Compound 4 binds to CF_1CF_0 -ATPase complex exerting a direct inhibition of the H^+ gradient dissipation and the Compounds 1 and 6–8 act as energy transfer inhibitors (H^+ -ATPase inhibitor) [17].

The electron-transport increase on the basal reaction up to 100% indicates that the compounds acted on the ATP–synthase complex, blocking the energy transfer or acting as proton-transfer decoupling. This behavior was observed for Compounds 1 and 6–8 through the increase of the basal step for Compound 4 by the increment of the basal and phosphorylating reactions [18,19].

To confirm if Compounds 1 and 6–8 act as energy-transfer inhibitors, and if Compound 4 acts as a decoupling agent, we performed H^+ -ATPase assays to verify their effect on the catalytic unit of the H^+ -ATPase complex (CF_0 - CF_1) [17]. Compounds 1 and 6–8 inhibited the energy transfer, as they decreased the inorganic phosphate (Pi) concentrations in the reaction medium by 25% at 100 μM and 300 μM , respectively. Corroborating the electron-transport data, both compounds are inhibitors of the CF_0 - CF_1 enzymatic site of the ATPase complex (Table 1). In its turn, Compound 4 increased Pi concentration by 18% at 100 μM , which confirmed its proton-gradient uncoupling profile.

Table 1. Effect of Compounds **1**, **4**, and **6–8** on inorganic phosphate (Pi).

Compound	(μM)	Pi (%)
Control	0	100
1	25	90
	50	78
	100	77
4	25	104
	50	108
	100	118
6–8	100	93
	200	88
	300	77

2.2. Uncoupled PSI and PSII Electron-Flow Determination

To localize the inhibition sites of the alkaloids on the thylakoid electron-transport chain, their effects on PSI and PSII (including partial reactions) were evaluated employing artificial donors and acceptors of electrons, as well as appropriate inhibitors [20]. Arborinine (**1**) inhibited uncoupled electron transport on PSII from water to DCBQ (from H_2O to Q_B) and the partial reactions from water to sodium silicomolybdate (SiMo) (from H_2O to Q_A) by 60% at 400 μM (Table 2). There were no significant results (<4%) for the reactions from DPC to 2,6-dichlorophenolindophenol (DCPIP) (from P_{680} to Q_B).

Table 2. Effects of arborinine (**1**) on photosynthetic electron transport on photosystem II (PSII). Note: DCPIP, 2,6-dichlorophenolindophenol.

(μM)	H_2O to DCBQ		H_2O to Sodium Silicomolybdate (SiMo)		DPC to DCPIP	
	<i>a</i>	<i>b</i>	<i>A</i>	<i>b</i>	<i>C</i>	<i>b</i>
0	547.5 \pm 2.74	100	511.0 \pm 2.56	100	256.0 \pm 1.28	100
50	-	-	-	-	283.0 \pm 1.42	110.6
100	401.5 \pm 2.00	74	328.5 \pm 1.64	65	268.0 \pm 1.34	104.5
200	292.0 \pm 1.46	54	255.5 \pm 1.28	50	268.0 \pm 1.34	104.5
300	255.5 \pm 1.28	47	237.3 \pm 1.19	47	-	-
400	219.0 \pm 1.09	40	219.0 \pm 1.09	43	-	-

a ($\mu\text{equiv e}^- \text{h}^{-1} \text{mg}^{-1} \text{Chl}^{-1}$), *b* (%), *c* ($\mu\text{M DCPIP}_{\text{red}} \text{mg}^{-1} \text{Chl}^{-1}$).

The polarographic measures indicated that **1** inhibited the passage from H_2O to Q_A , that is, on both sides of the electron transport on PSII. The first inhibition site (H_2O to SiMo) occurs in the enzyme where water photo-oxidation happens, and the other at DPC (donates electron at P_{680}) to DCPIPox (accepts electrons at Q_B site), located at the water-splitting enzyme complex (OEC) and between the range of electron flow from P_{680} to Q_A . These results indicated that **1** inhibited PSII at the span of electron transport from H_2O to Q_A due the fact that SiMo accepts electrons exactly at the Q_A site. Table 2 shows that the span of electron transport from P_{680} to Q_B was not inhibited in all concentrations. Compound **1** inhibited the PSI uncoupled electron transport from reduced DCPIP to MV by 50% at 200 μM (Table 3). However, no changes were observed on inhibitory activity at higher concentrations.

Table 3. Effects of arborinine (**1**) on photosynthetic uncoupled electron transport at PSI.

(μM)	DCPIP _{red} a Methylviologen (MV)	
	<i>a</i>	<i>b</i>
0	1467.4 \pm 7.34	100
100	867.1 \pm 4.34	59.1
200	733.7 \pm 3.67	50
400	667.0 \pm 3.34	46

a ($\mu\text{equiv e}^- \text{h}^{-1} \text{mg}^{-1} \text{Chl}^{-1}$) *b* (%).

2.3. Chl *a* Fluorescence Measurements in Spinach Leaf Discs

The Chl *a* fluorescence assay is a widely used tool to evaluate the photosynthetic apparatus in plants submitted to different stresses, as well as to provide detailed information about the structure and function of PSII [10,20]. For this experiment, all alkaloids were evaluated at 150 and 300 μM . Compounds **1–4** showed very low activity during the experiment, less than 20% compared to negative control (data not shown).

Compound **5** increased dV/dt_0 and decreased PI_{abs} , both parameters by 60% at 150 μM , which represents a stressful event occurring in the plant. The association of these parameters suggests that the natural redox process of photosynthesis was interfered with (Figure 3A). Parameters PSI_0 , $PHI(E_0)$, Sm , ET_0/CS_0 , and ET_0/RC were reduced by 40%, which directly represents that electron transport on the redox process was interrupted, indicating damage to PSII. The decrease in Sm demonstrates that not all absorbed energy was used, and then it was eliminated from the process. Energy dissipation was confirmed through the increase of the nonphotochemical “de-excitation” constant (Kn) by 40% and the quantum yield ($t = 0$) of dissipation energy ($PHI(D_0)$) by 20%. Thus, the energy contained in the system was released as heat or transferred to another molecule.

Compounds **6–8** were active at both concentrations during the leaf-disc fluorescence assay (Figure 3A,B). The PI_{abs} parameter showed a decrease of 70% at 150 μM , indicating a nontraditional photosynthesis process. Parameters PSI_0 , $PHI(E_0)$, ET_0/CS_0 and ET_0/RC were reduced by 40, 40, 60 and 40%, respectively, at 150 μM . These decrements represent damage in electron transport on PSII, showing that the calculated quantum-yield values for the electron transport decreased in the process of the flux being inhibited. The reduction of ET_0/CS_0 , ET_0/RC , and RC/CS_0 parameters by 30% indicated that the electron transport was being blocked, as well as a reduction in reaction centers participating in the process. Like Compound **5**, the increment was promoted by the mixture of analogs on the dV/dt_0 , SmK , Kn , and $PHI(D_0)$ parameters.

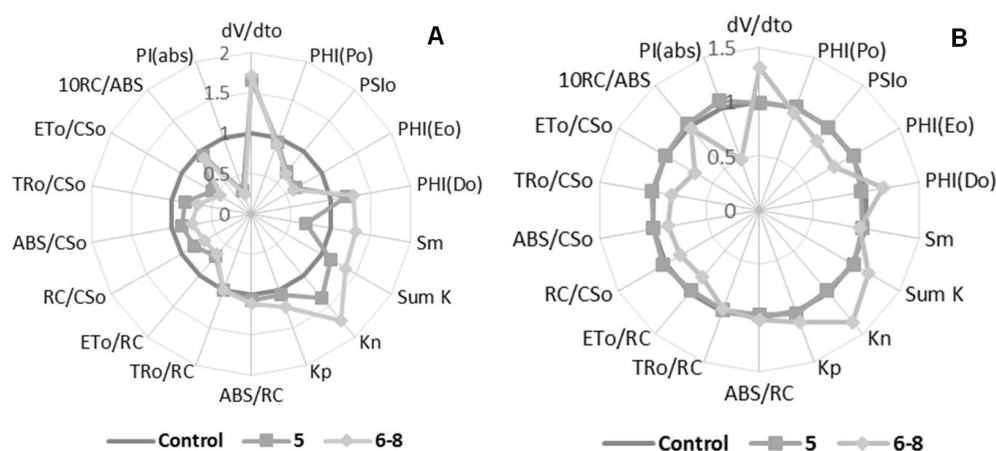


Figure 3. Radar plot of Compounds **5** and **6–8** effects on Chl *a* fluorescence parameters calculated from an *OJIP* transient curve. Panel (A) 150 μM , and Panel (B) 300 μM .

A *J* band (2 ms) was observed at the *OJIP* transient curve for Compound 5 (150 μ M), which indicates inhibition at the quinone level, on the acceptor side of PSII (Figure 4A). An increase at *J* step can be understood as evidence for reduced-form QA accumulation (QA^-) due electron-transport deceleration beyond QA [21]. Since the PSII electron flux was inhibited, the maximum PSII microelectrons field carries less QA^- . This aspect corroborated the reduction of the PSI_0 and $PHI(E_0)$ quantum parameters. The results of the fluorescence emission on spinach-leaf discs confirm the in vitro electron transport results, which revealed Compound 5 acting as a Hill reaction inhibitor.

The same *J* band was observed when the mixture of quinolone alkaloids was submitted to the assays (Figure 4B), which confirms that Compounds 6–8 also behave like 3-(3,4-dichlorophenyl)-1,1-dimethylurea (DCMU), inhibiting the acceptor side of the PSII [10]. The Chl *a* experiment also showed the appearance of the *I* band near 30 ms (Figure 4C), which exclusively refers to the efficiency of the quinone pool. This event indicates whether plastoquinones are active or not during the QA reduction process. When the *I* band is found in negative values (on the graph), it suggests that the QA pool is functioning excellently, and an increase in the *J* band is also observed, that is, this indicates that the interaction site is the reaction center (P680). The transient bands show exactly this effect (Figure 4A,B). Phase *I* appears when a dynamic equilibrium is reached between the reduction of the plastoquinone pool by the electron flow from the PSII and its oxidation due to PSI activity [22].

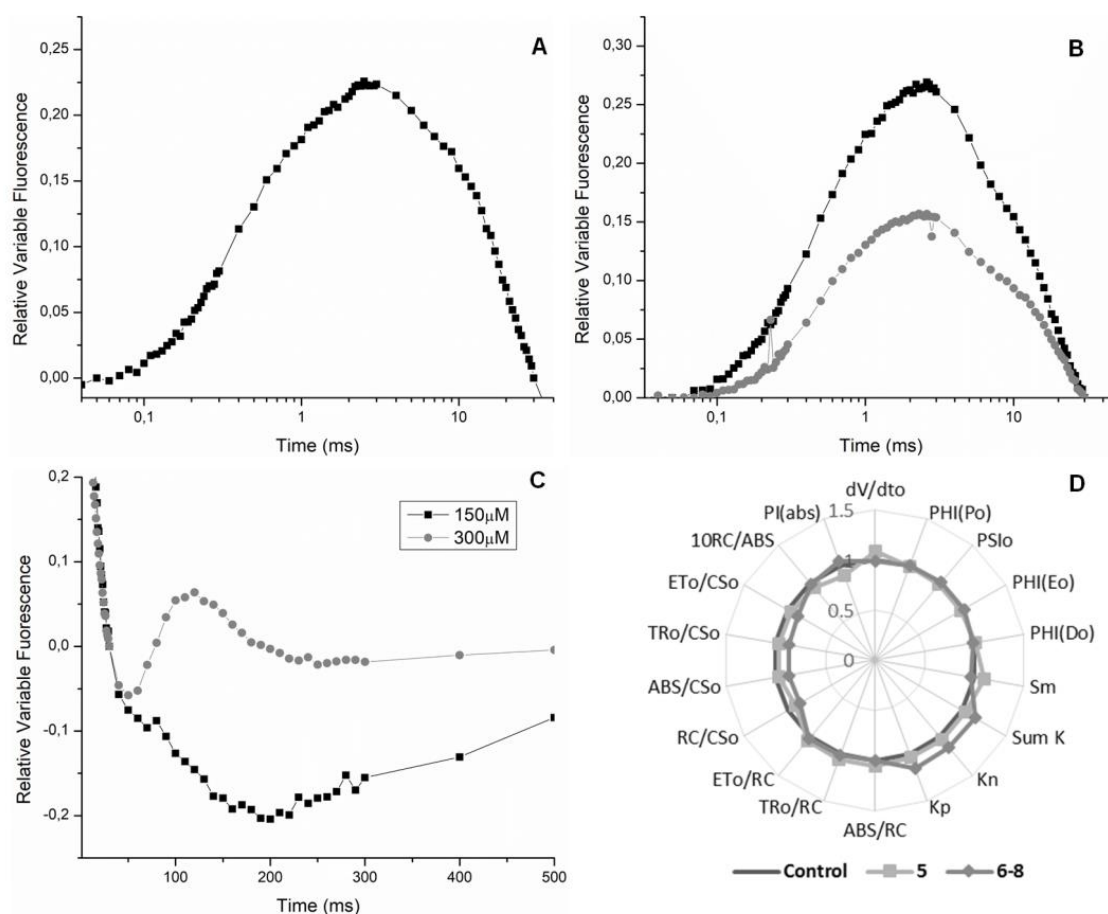


Figure 4. Panel (A) Appearance of the *J*-band in the presence of Compound 5 at 150 μ M. Panel (B) Appearance of the *J*-band in the presence of Compounds 6–8 at 150 and 300 μ M. Panel (C) Appearance of the *I*-band in the presence of 6–8 at 150 and 300 μ M. Panel (D) Radar plot of Compounds 5 and 6–8 effects on Chl *a* fluorescence parameters calculated from *OJIP* curve of sprayed *Lolium perenne* plants after 72 h.

2.4. In Vivo Assays: Chl *a* Fluorescence Determination in Intact *L. Perenne* Leaves

The in vivo Chl *a* fluorescence experiment represents a powerful tool to evaluate the performance of the photosynthesis system in living plants without causing any damage to them [23]. To evaluate compound activity, solutions at 150 and 300 μM were sprayed on the leaves of *L. perenne* plants. However, only Compound 5 and the mixture 6–8 were tested because they presented the best results on a semivivo assay. After 24, 48, and 72 h of treatment, Chl *a* fluorescence transients were measured and the OJIP parameters were calculated employing Biolyser HP software.

Data showed that 5 and 6–8 on plants after 24 and 48 h were insignificant, but a small variation on photosynthetic parameters was observed after 72 h at 150 μM (Figure 4D). In short, the in vivo results are less significant than the results observed on the semivivo assay. We justify this because there are many natural obstacles that the compounds have to transcend to reach their target (the chloroplast), for example, cell walls and membranes [23].

2.5. Dry Biomass Determination

Dry biomass results were obtained using *L. perenne* plants 15 days after compound application. Compound 5 and the mixture 6–8 were evaluated at 150 and 300 μM . The other compounds were not tested, as they did not present any activity in the previously assays. DCMU, a herbicide, was used as positive control (Table 4). Fortunately, the best results were observed for the lowest concentration, 150 μM . Treatments 5 and 6–8 decreased dry biomass by 20% and 23%, respectively, compared to negative control. These are significant results since they behaved like DCMU, which reduced 23% of the biomass of the target plant.

Table 4. Dry biomass assay for Compounds 5 and 6–8. Note: DCMU, 3-(3,4-dichlorophenyl)-1,1-dimethylurea.

Treatment	(μM)	Dry Biomass (mg)	Percentage (%)
Control	0	400.0 \pm 2.00	100
DCMU	10	307.0 \pm 1.54	77
5	150	320.0 \pm 1.60	80
	300	327.0 \pm 1.64	82
6–8	150	310.0 \pm 1.55	77
	300	350.0 \pm 1.75	87

Based on in vitro, semivivo, and in vivo approaches, Compound 5 acts as a photosynthetic electron-transport inhibitor and as a plant-growth regulator. Mixture 6–8, on the other hand, acts as an electron-transport and energy-transfer inhibitor, as well as plant-growth regulator. Our results showed that almost all alkaloids behaved as photosynthesis inhibitors once some of them acted as Hill reaction inhibitors. Through fluorescence measurement, we could observe the presence of transient bands *J* and *I* (obtained from OJIP-test). These steps suggest that compounds isolated from *R. graveolens* inhibited electron flow on the acceptor side of PSII, exactly like DCMU does. Therefore, the aim of our work was to present that natural products still could be employed on programs to lead to new scaffold models for herbicides in the future, since natural products remains an interesting alternative to replace the commercial herbicides.

3. Materials and Methods

3.1. Alkaloid Isolation from *Ruta Graveolens*

The ethanolic extract (203.6 g) from *Ruta graveolens* leaves was solubilized in $\text{CH}_3\text{OH}:\text{H}_2\text{O}$ (1:3, *v:v*) and extracted by liquid–liquid partition with hexane and dichloromethane to obtain the partitioned extract fractions.

The dichloromethane fraction (14.6 g) from *Ruta graveolens* leaves was subjected to a chromatographic column using silica gel 60 (70–230 mesh), employing as a mobile phase increasing hexane, dichloromethane, acetone, and methanol concentrations to obtain 6 fractions (1–6). Fraction 5 (0.746 g) was subjected to a new chromatographic procedure using Sephadex LH-20 with isocratic elution formed by dichloromethane:methanol (1:1, *v:v*) to afford arborinine (**1**, 18.4 mg) and 1,4-dihydroxy-2,3-dimethoxy-*N*-methylacridone (**2**, 16.5 mg) [24].

1-hydroxy-3-methoxy-*N*-methylacridone (**3**, 17.9 mg) was obtained from the dichloromethane:hexane fraction of *Ruta graveolens* leaves using silica gel (70–230 mesh) and solvents of increasing polarity (hexane, dichloromethane, acetone, and methanol), followed by a second chromatographic purification over Sephadex LH-20 with isocratic elution dichloromethane: methanol (1:1, *v:v*) [25].

From the methanol fraction of *Ruta graveolens* leaves, the *N*-methyl-4-methoxy-2-quinolone (**4**, 19.3 mg) and graveoline (**5**, 14.1 mg) compounds were purified using a chromatographic column with silica gel as support, and hexane, dichloromethane, acetone, and methanol as the mobile phase [26].

The ethanolic extract (7.0 g) from the *Ruta graveolens* roots was solubilized with methanol:water (1:3 *v:v*), and subjected to liquid–liquid extraction with hexane to provide the respective fraction (1.53 g). The hexanic fraction was subjected to purification using silica gel (70–230 mesh). The mobile phase was composed of increasing portions of hexane, dichloromethane, acetone, and methanol to obtain 8 fractions (I–VIII). Fraction II (0.105 g) was subjected to new chromatographic purification by Sephadex LH-20 with isocratic elution dichloromethane:methanol (3:7, *v:v*) to obtain a homolog mixture of **6**, **7**, and **8**. The mixture was analyzed with GC-MS. The instrument was set to an initial temperature of 150 °C, and maintained at that temperature for 1 min. At the end of this period, the oven temperature was increased to 300 °C, at the rate of 10 °C/min, and maintained for 20 min. The chromatogram presented 3 peaks at retention times (t_R) 11.5 min (**6**, m/z 313), 12.0 min (**7**, m/z 327), and 13.0 min (**8**, m/z 341). Based on the GC-MS experiment, a ratio of 8:1:1 (based on the peak areas) was estimated for **6**, **7**, and **8** [27].

Compound 1. $^1\text{H-NMR}$ (200 MHz, CDCl_3) δ : 3.81 (s, 3H, *N*-Me), 3.92 (s, 3H, 3-OMe), 4.00 (s, 3H, 2-OMe), 6.23 (s, 1H, H-4), 7.23 (ddd, $J = 8.0, 6.8$ and 0.7 Hz, 1H, H-7), 7.50 (dl, $J = 8.0$ Hz, 1H, H-5), 7.73 (ddd, $J = 8.0, 6.8$ and 1.4 Hz, 1H, H-6), 8.42 (dd, $J = 8.0$ and 1.4 Hz, 1H, H-8), 14.75 (s, 1H, OH). $^{13}\text{C-NMR}$ (100 MHz, CDCl_3) δ : 34.1 (*N*-Me), 56.0 (C3-OMe), 60.8 (C2-OMe), 86.8 (C-4), 105.8 (C-9a), 114.5 (C-5), 120.8 (C-8a), 121.5 (C-7), 126.2 (C-8), 130.2 (C-2), 134.6 (C-6), 140.5 (C-4a), 142.0 (C-5a), 156.2 (C-1), 159.3 (C-3), 180.8 (C-9).

Compound 2. $^1\text{H-NMR}$ (200 MHz, CDCl_3) δ : 3.96 (s, 3H, *N*-Me), 3.99 (s, 3H, 2-OMe), 4.03 (s, 3H, 3-OMe), 7.32 (ddd, $J = 8.0, 7.5$ and 1.6 Hz, 1H, H-7), 7.48 (dl, $J = 8.7$ Hz, 1H, H-5), 7.76 (ddd, $J = 8.7, 7.5$ and 1.6 Hz, 1H, H-6), 8.36 (dd, $J = 8.7$ and 1.6 Hz, 1H, H-8), 14.69 (s, 1H, 1-OH). $^{13}\text{C-NMR}$ (50 MHz, CDCl_3) δ : 44.0 (*N*-Me), 61.0 (C2-OMe), 61.5 (C3-OMe), 109.4 (C-9a), 116.6 (C-5), 121.3 (C-8a), 122.1 (C-8), 126.2 (C-7), 134.6 (C-6), 134.7 (C-2), 140.0 (C-3), 146.1 (C-5a), 151.5 (C-4), 155.8 (C-1), 157.0 (C-4a), 182.3 (C-9).

Compound 3. $^1\text{H-NMR}$ (200 MHz, CDCl_3) δ : 3.77 (s, 3H, *N*-Me), 3.90 (s, 3H, OMe), 6.30 (s, 2H, H-2 and H-4), 7.30 (ddd, $J = 8.0, 7.2$ and 1.6 Hz, 1H, H-7), 7.40 (dl, $J = 8.0$ Hz, 1H, H-5), 7.73 (ddd, $J = 8.0, 7.2$ and 1.6 Hz, 1H, H-6), 8.44 (dd, $J = 8.0$ and 1.6 Hz, 1H, H-8), 14.75 (s, 1H, OH), $^{13}\text{C-NMR}$ (50 MHz, CDCl_3) δ : 33.3 (*N*-Me), 55.6 (OMe), 90.1 (C-4), 94.1 (C-2), 105.0 (C-9a), 114.4 (C-5), 121.0 (C-8a), 121.4 (C-7), 126.7 (C-8), 134.1 (C-6), 142.0 (C-5a), 144.0 (C-4a), 166.0 (C-1), 166.1 (C-3), 180.0 (C-9).

Compound 4. $^1\text{H-NMR}$ (200 MHz, CDCl_3) δ : 3.64 (s, 3H, *N*-Me), 3.92 (s, 3H, OMe), 6.23 (s, 1H, H-3), 7.96 (dd, $J = 8.0$ and 1.5 Hz, 1H, H-5), 7.21 (ddd, $J = 8.0$, 7.1 and 1.5 Hz, 1H, H-6), 7.34 (dl, $J = 8.0$ Hz, 1H, H-8), 7.58 (ddd, $J = 8.0$, 7.1 and 1.5 Hz, 1H, H-7). $^{13}\text{C-NMR}$ (50 MHz, CDCl_3) δ : 28.8 (*N*-Me), 55.3 (OMe), 96.1 (C-3), 113.8 (C-8), 116.2 (C-4a), 121.4 (C-6), 123.1 (C-5), 131.0 (C-7), 139.4 (C-8a), 162.4 (C-4), 163.6 (C-2).

Compound 5. $^1\text{H-NMR}$ (400 MHz, CDCl_3) δ : 3.59 (s, 3H, *N*-Me), 5.99 (s, 2H, H-7'), 6.26 (s 1H, H-3), 6.78 (dd, $J = 1.6$ and 0.4 Hz, 1H, H-2'), 6.81 (dd, $J = 8.0$ and 1.6 Hz, 1H, H-6'), 6.84 (dd, $J = 8.0$ and 0.4 Hz, 1H, H-5'), 7.34 (ddd, $J = 8.0$, 6.8 and 1.6 Hz, 1H, H-6), 7.49 (dl, $J = 8.4$ Hz, 1H, H-8), 7.64 (ddd, $J = 8.4$, 6.8 and 1.6 Hz, 1H, H-7), 8.37 (dd, $J = 8.0$ and 1.6 Hz, 1H, H-5).

Compounds 6–8. $^1\text{H-NMR}$ (400 MHz, CDCl_3) δ : 0.87 (t, $J = 8.0$ Hz, 3H, CH_3 -9'), 1.26–2.37 (2H-2' to 2H-8', overlapping with the signals of 7 and 8), 3.05 (qt, $J = 8.0$ Hz, 2H, H-1'), 4.12 (s, 3H, *N*-Me), 6.70 (s, 1H, H-3), 7.54 (tl, $J = 8.0$ Hz, 1H, H-8), 7.77 (tl, $J = 8$ Hz, 1H, H-6), 8.19 (tl, $J = 8.0$ Hz, 1H, H-5), 8.19 (tl, $J = 8.0$ Hz, 1H, H-7).

3.2. Chloroplast Isolation and Chlorophyll Quantitative Determination

Intact chloroplasts were isolated from spinach leaves (*Spinacea oleracea* L.), as previously described [12,22,25]. Chlorophyll concentration was measured spectrophotometrically through a chloroplast suspension in a solution of 400 mM sucrose, 5 mM MgCl , 10 mM KCl, 30 mM tricine-KOH, and pH 8.0 [12].

3.3. Measurement of Noncyclic Electron Transport Rate

The light-induced noncyclic electron-transport activity from water to MV was determined polarographically employing a Clark-type electrode in the presence of 50 μM of MV [19]. Basal electron transport was quantified by illuminating a solution of chloroplasts (20 μg Chl/mL) in 3 mL of 100 mM sorbitol, 10 mM KCl, 5 mM MgCl_2 , 0.5 mM KCN, 15 mM tricine-KOH, and 50 μM MV at pH 8.0 for 1 min. The phosphorylating electron-transport rate was estimated for the basal electron transport from water to MV, adding 1 mM of ADP and 3 mM KH_2PO_4 . In turn, uncoupled electron transport was evaluated in the same solution used for basal step, with 6 mM NH_4Cl added as an uncoupler [12].

3.4. Uncoupled PSI and PSII Electron-Flow Determination

Electron-flow activities were monitored by an oxygen monitor yellow spring instrument model 5300A using a Clark-type electrode. All reaction mixtures were illuminated with filtered light (5 cm filter of 1% CuSO_4 solution) from a projector lamp (GAF 2660) at room temperature. For each reaction, a blank experiment was performed with chloroplasts in the reaction medium. Uncoupled PSII from H_2O to DCPIP was measured through the reduction of DCPIP-supported O_2 evolutions, monitored polarographically. The reaction medium for assaying PSII activity was composed by the same basal electron-transport medium, but in the presence of 1 μM 2,5-dibromo-3-methyl-6-isopropyl-1,4-*p*-benzoquinone (DBMIB), 100 μM DCPIP, and 300 μM $\text{K}_3[\text{Fe}(\text{CN})_6]$ and 6 mM NH_4Cl [28].

To determine the uncoupled partial reaction of PSII from water to SiMo, solutions of 200 μM of SiMo and 10 μM of DCMU were added to the solution used for the PSII reactions (3 mL), then chloroplasts (20 μg Chl/mL) were added and illuminated for 1 min [29].

Uncoupled PSI electron transport from the reduced DCPIP with sodium ascorbate to MV was determined in a similar form in a basal noncyclic electron-transport medium. However, the following reagents were added: 10 μM DCMU, 100 μM DCPIP, 50 μM MV, 300 μM sodium ascorbate, and 6 mM NH_4Cl [30]. All measurements were performed in triplicate and compared to negative control (solvent, dimethyl sulfoxide (DMSO)).

3.5. H^+ -ATPase Activity Measurements

Intact chloroplasts isolated from *S. oleracea* L. were resuspended in a solution of 0.35 M sorbitol, 2 mM EDTA, 1 mM $MgCl_2 \cdot 6H_2O$, 1 mM $MnCl_2$, and 50 mM Hepes medium at pH 7.6. H^+ -ATPase activity was measured as reported [24]. NH_4Cl and DMSO were employed as positive and negative controls, respectively. Pi was quantified using a UV spectrophotometer with measurements in $\lambda = 660$ nm.

3.6. Chlorophyll A Fluorescence Measurements in Spinach-Leaf Discs

Ten 7 mM leaf discs were placed in Petri dishes with 10 mL of a modified Krebs medium containing 115 mM NaCl, 5.9 mM KCl, 1.2 mM $MgCl_2$, 1.2 mM KH_2PO_4 , 1.2 mM Na_2SO_4 , 2.5 mM $CaCl_2$, and 25 mM $NaHCO_3$ (pH 7.4). The Petri dishes were maintained in orbital stirring for 12 h at room temperature. All alkaloids, 1–8, were added to the system for a new period of stirring (12 h). The discs were dark-adapted for 30 min and chlorophyll *a* fluorescence was measured at room temperature through a Hansatech Fluorescence Handy PEA (Plant Efficiency Analyzer, King's Lynn, UK) [16,25].

3.7. Plant Material for In Vivo Assays

A suspension of *Lolium perenne* seeds prepared with 10% sodium hypochlorite solution was kept in an orbital shaker for 15 min. Then, the sodium hypochlorite solution was removed and the seeds were washed 3 times with distilled water; 100 seeds were placed in 12 cm diameter pots containing a mixture of 50:25:25 (*w/w/w*) soil/peat-moss/agrolite. All pots were watered daily and maintained in a greenhouse at 25–30 °C under normal day/night illumination (12/12 h). *L. perenne* plants were selected by uniformity after being 15 days old. The plants were separated in 3 groups: negative control (DMSO), positive control (50 μ M of DCMU), and plants treated with each alkaloid at 150 and 300 μ M [12] by being manually sprayed.

3.8. Chlorophyll a Fluorescence Determination in Intact *L. Perenne* Leaves and Dry Biomass Determination

Chl *a* fluorescence was measured in leaves from the control plants and those treated with alkaloids 1–8 at 150 and 300 μ M. After 24, 48, and 72 h of spraying, the leaves that adapted to the dark for 15 min were excited by light from an array of 3 light-emitting diodes delivering 3000 μ mol $m^{-2} s^{-1}$ of red light (650 nm). The Chl *a* fluorescence induction curves were measured at room temperature with a portable Hansatech Fluorescence Handy PEA apparatus. Photosynthetic parameters like as PI_{abs} , dV/dt_0 , Sm, ABS/RC, TR_0/RC , ET_0/RC , TR_0/ABS , ET_0/TR_0 , ET_0/ABS , $\Phi(D_0)$, ABS/CS_0 , TR_0/CS_0 , ET_0/CS_0 , k_p , k_n , and Sumk were represented in a radar plot [12]. For the dry-biomass experiment, 15 days old *L. perenne* plants treated with alkaloids 1–8 at 150 and 300 μ M were dried in an oven at 65 °C to reach a constant weight. Then, the dry biomass was measured using analytical balance [12].

Author Contributions: Conceptualization, T.A.M.V., B.L.-H. and O.M.S.; Methodology, B.S.B., O.M.S. and B.K.-D.; Software, L.C.C.V.; Validation, O.M.S. and B.K.-D.; Formal Analysis, B.S.B., O.M.S., T.A.M.V. and B.K.-D.; Investigation, O.M.S.; Resources, M.F.d.G.F.d.S. and B.L.-H.; Data Curation, O.M.S., T.A.M.V., L.C.C.V. and B.K.-D.; Writing-Original Draft Preparation, O.M.S.; Writing-Review and Editing, O.M.S., T.A.M.V. and L.C.C.V.; Visualization, O.M.S., T.A.M.V. and L.C.C.V.; Supervision, T.A.M.V., B.L.-H. and M.F.d.G.F.d.S.; Project Administration, B.L.-H. and M.F.d.G.F.d.S.; Funding Acquisition, B.L.-H. and M.F.d.G.F.d.S.

Funding: The authors gratefully acknowledge financial support from Grants DGAPA-UNAM, IN 205806; CNPq, and CAPES—Finance Code 001.

Acknowledgments: Olívia Moreira Sampaio thanks FAPESP (Fundação de Amparo a Pesquisa do Estado de São Paulo-Brazil) for the scholarship support.

Conflicts of Interest: The authors declare no conflict of interest.

Abbreviations

ATP	adenosine triphosphate
Chl	chlorophyll
DBMIB	2,5-dibromo-3-methyl-6-isopropyl-1,4- <i>p</i> -benzoquinone
DCMU	3-(3,4-dichlorophenyl)-1,1-dimethylurea
DCPIP	2,6-dichlorophenolindophenol
DMSO	dimethyl sulfoxide
MV	methylviologen
NADPH	dihydrinicotinamide-adenine dinucleotide phosphate
Pi	inorganic phosphate
PSI	photosystem I
PSII	photosystem II
RC	reaction center
SiMo	sodium silicomolybdate

References

1. De Feo, V.; De Simone, F.; Senatore, F. Potential allelochemicals from the essential oil of *Ruta graveolens*. *Phytochemistry* **2002**, *61*, 573–578. [[CrossRef](#)]
2. Hale, A.L.; Meepagala, K.M.; Oliva, A.; Aliotta, G.; Duke, S.O. Phytotoxins from the leaves of *Ruta graveolens*. *J. Agric. Food Chem.* **2004**, *52*, 3345–3349. [[CrossRef](#)] [[PubMed](#)]
3. Kuzovkina, I.; Al'terman, I.; Schneider, B. Specific accumulation and revised structures of acridone alkaloid glucosides in the tips of transformed roots of *Ruta graveolens*. *Phytochemistry* **2004**, *65*, 1095–1100. [[CrossRef](#)] [[PubMed](#)]
4. Wansi, J.D.; Wandji, J.; Mbaze Meva'a, L.; Kamdem Waffo, A.F.; Ranjit, R.; Khan, S.N.; Asma, A.; Iqbal, C.M.; Lallemand, M.-C.; Tillequin, F.; Fomum-Tanee, Z. Alpha-glucosidase inhibitory and antioxidant acridone alkaloids from the stem bark of *Orixiopsis glaberrima* ENGL. (Rutaceae). *Chem. Pharm. Bull.* **2006**, *54*, 292–296. [[CrossRef](#)] [[PubMed](#)]
5. Michael, J.P. Quinoline, quinazoline and acridone alkaloids. *Nat. Prod. Rep.* **2007**, *24*, 223. [[CrossRef](#)] [[PubMed](#)]
6. Musiol, R.; Serda, M.; Hensel-Bielowka, S.; Polanski, J. Quinoline-Based Antifungals. *Curr. Med. Chem.* **2010**, *17*, 1960–1973. [[CrossRef](#)] [[PubMed](#)]
7. Lacroix, D.; Prado, S.; Kamoga, D.; Kasenene, J.; Bodo, B. Structure and in vitro antiparasitic activity of constituents of *Citropsis articulata* root bark. *J. Nat. Prod.* **2011**, *74*, 2286–2289. [[CrossRef](#)] [[PubMed](#)]
8. Torres-Romero, D.; King-Díaz, B.; Strasser, R.J.; Jiménez, I.A.; Lotina-Hennsen, B.; Bazz-Cchi, I.L. Friedelane triterpenes from *celastrus vulcanicola* as photosynthetic inhibitors. *J. Agric. Food Chem.* **2010**, *58*, 10847–10854. [[CrossRef](#)] [[PubMed](#)]
9. Menezes-De-Oliveira, D.; Aguilar, M.I.; King-Díaz, B.; Vieira-Filho, S.A.; Pains-Duarte, L.; De Fátima Silva, G.D.; Lotina-Hennsen, B. The triterpenes 3 β -Lup-20(29)-en-3-ol and 3 β -Lup-20(29)-en-3-yl acetate and the carbohydrate 1,2,3,4,5,6-hexa-O-acetyl-dulcitol as photosynthesis light reactions inhibitors. *Molecules* **2011**, *16*, 9939–9956. [[CrossRef](#)] [[PubMed](#)]
10. Sampaio, O.M.; de Castro Lima, M.M.; Veiga, T.A.M.; King-Díaz, B.; da Silva, M.F.d.G.F.; Lotina-Hennsen, B. Evaluation of antidesmone alkaloid as a photosynthesis inhibitor. *Pestic. Biochem. Phys.* **2016**, *134*, 55–62. [[CrossRef](#)] [[PubMed](#)]
11. Andreiadis, E.S.; Chavarot-Kerlidou, M.; Fontecave, M.; Artero, V. Artificial photosynthesis: From molecular catalysts for light-driven water splitting to photoelectrochemical cells. *Photochem. Photobiol.* **2011**, *87*, 946–964. [[CrossRef](#)] [[PubMed](#)]
12. McConnell, I.; Li, G.H.; Brudvig, G.W. Energy Conversion in Natural and Artificial Photosynthesis. *Chem. Biol.* **2010**, *17*, 434–447. [[CrossRef](#)] [[PubMed](#)]
13. Chen, S.; Zhou, F.; Yin, C.; Strasser, R.J.; Yang, C.; Qiang, S. Application of fast chlorophyll a fluorescence kinetics to probe action target of 3-acetyl-5-isopropyltetramic acid. *Environ. Exp. Bot.* **2011**, *73*, 31–41. [[CrossRef](#)]
14. Strasser, R.J.; Srivastava, A. Govindjee polyphasic chlorophyll a fluorescence transient in plants and cyanobacteria. *Photochem. Photobiol.* **1995**, *61*, 32–42. [[CrossRef](#)]

15. Hasan, C.; Ahmed, N.; Haque, R.; Haque, M.; Begum, S.; Sohrab, M.; Ahsan, M. Secondary metabolites from the stem of *Ravenia spectabilis* Lindl. *Pharmacogn. Mag.* **2013**, *9*, 76. [[CrossRef](#)] [[PubMed](#)]
16. Spatafora, C.; Tringali, C. Bioactive metabolites from the bark of *Fagara macrophylla*. *Phytochem. Anal.* **1997**, *8*, 139–142. [[CrossRef](#)]
17. Macías-Rubalcava, M.L.; García-Méndez, M.C.; King-Díaz, B.; Macías-Ruvalcaba, N.A. Effect of phytotoxic secondary metabolites and semisynthetic compounds from endophytic fungus *Xylaria feejeensis* strain SM3e-1b on spinach chloroplast photosynthesis. *J. Photochem. Photobiol. B Biol.* **2017**, *166*, 35–43. [[CrossRef](#)] [[PubMed](#)]
18. Hernández-Terrones, M.G.; Aguilar, M.I.; King-Díaz, B.; Lotina-Hennsen, B. Interference of methyl trachyloban-19-oate ester with CF₀ of spinach chloroplast H⁺-ATPase. *Arch. Biochem. Biophys.* **2003**, *418*, 93–97. [[CrossRef](#)]
19. Xiang, M.; Chen, S.; Wang, L.; Dong, Z.; Huang, J.; Zhang, Y.; Strasser, R.J. Effect of vulculic acid produced by *Nimbya alternantherae* on the photosynthetic apparatus of *Alternanthera philoxeroides*. *Plant Physiol. Biochem.* **2013**, *65*, 81–88. [[CrossRef](#)] [[PubMed](#)]
20. Paunov, M.; Koleva, L.; Vassilev, A.; Vangronsveld, J.; Goltsev, V. Effects of different metals on photosynthesis: Cadmium and zinc affect chlorophyll fluorescence in durum wheat. *Int. J. Mol. Sci.* **2018**, *19*. [[CrossRef](#)] [[PubMed](#)]
21. Marchi, G.; Marchi, E.C.S.; Wang, G.; McGiffen, M. Effect of age of a sorghum-sudangrass hybrid on its allelopathic action. *Planta Daninha* **2008**, *26*, 707–716. [[CrossRef](#)]
22. King-Díaz, B.; Dos Santos, F.J.L.; Rubinger, M.M.M.; Piló-Veloso, D.; Lotina-Hennsen, B. A diterpene γ -lactone derivative from *Pterodon polygalaeflorus* Benth. as a photosystem II inhibitor and uncoupler of photosynthesis. *Z. Naturforsch. C* **2006**, *61*, 227–233. [[CrossRef](#)] [[PubMed](#)]
23. Castelo-Branco, P.; Santos, F.J.L.; Rubinger, M.; Ferreira-Alves, D.; Piló-Veloso, D.; King, B.; Lotina-Hennsen, B. Inhibition and uncoupling of photosynthetic electron transport by diterpene lactone amide derivatives. *Z. Naturforsch. C* **2008**, *63*. [[CrossRef](#)]
24. Min, Y.D.; Kwon, H.C.; Yang, M.C.; Lee, K.H.; Choi, S.U.; Lee, K.R. Isolation of limonoids and alkaloids from *Phellodendron amurense* and their multidrug resistance (MDR) reversal activity. *Arch. Pharm. Res.* **2007**, *30*, 58–63. [[CrossRef](#)] [[PubMed](#)]
25. Seya, K.; Furukawa, K.-I.; Chiyoya, M.; Yu, Z.; Kikuchi, H.; Daitoku, K.; Motomura, S.; Murakami, M.; Oshima, Y.; Fukuda, I. 1-Methyl-2-undecyl-4(1H)-quinolone, a derivative of quinolone alkaloid evocarpine, attenuates high phosphate-induced calcification of human aortic valve interstitial cells by inhibiting phosphate cotransporter PiT-1. *J. Pharmacol. Sci.* **2016**, *131*, 51–57. [[CrossRef](#)] [[PubMed](#)]
26. Yruela, I.; Montoya, G.; Alonso, P.; Picorel, R. Identification of the Pheophytin-QA-Fe domain of the reducing side of the photosystem II as the Cu(II)-inhibitory binding site. *J. Biol. Chem.* **1991**, *266*, 22847–22850. [[PubMed](#)]
27. Giaquinta, R.T.; Dille, R.A. A partial reaction in Photosystem II: Reduction of silicomolybdate prior to the site of dichlorophenyldimethylurea inhibition. *Bioenergetics* **1975**, *387*, 288–305. [[CrossRef](#)]
28. Garza-Ortiz, A.; King-Díaz, B.; Sosa-Torres, M.E.; Lotina-Hennsen, B. Interference of ruthenium red analogues at photosystem II of spinach thylakoids. *J. Photochem. Photobiol. B Biol.* **2004**, *76*, 85–94. [[CrossRef](#)] [[PubMed](#)]
29. Mills, J.D.; Mitchell, P.; Schürmann, P. Modulation of coupling factor ATPase activity in intact chloroplasts: The role of the thioredoxin system. *FEBS Lett.* **1980**, *112*, 173–177. [[CrossRef](#)]
30. Aguilar, M.I.; Romero, M.G.; Chávez, M.I.; King-Díaz, B.; Lotina-Hennsen, B. Biflavonoids isolated from *Selaginella lepidophylla* inhibit photosynthesis in spinach chloroplasts. *J. Agric. Food Chem.* **2008**, *56*, 6994–7000. [[CrossRef](#)] [[PubMed](#)]

Sample Availability: Samples of the compounds are not available from the authors.



© 2018 by the authors. Licensee MDPI, Basel, Switzerland. This article is an open access article distributed under the terms and conditions of the Creative Commons Attribution (CC BY) license (<http://creativecommons.org/licenses/by/4.0/>).